AD-A136 247 ION BEAM ASSISTED DEPOSITION OF SIO2(U) NEW MEXICO UNIV 1/1
ALBUQUERQUE INST FOR MODERN OPTICS J R MCNEIL 1983
AFOSR-TR-83-1220 AFOSR-82-0165

UNCLASSIFIED F/G 20/7 NL

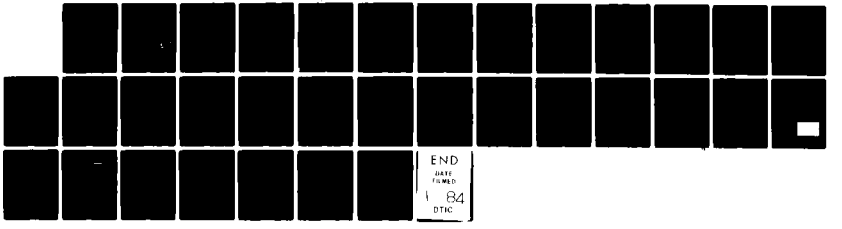

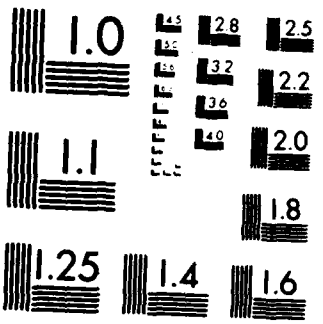

AFOSR-TR- 83-1220

(12)

Final Report Submitted to

Air Force Office of Scientific Research

by

The University of New Mexico
Institute for Modern Optics
Department of Electrical and
Computer Engineering
Albuquerque, New Mexico 87131

ION BEAM ASSISTED DEPOSITION OF SiO_2

GRANT NUMBER AFOSR-82-0165

Principal Investigator: John R. McNeil
Assistant Professor of
Electrical Engineering
University of New Mexico

Unclassified

SECURITY CLASSIFICATION OF THIS PAGE (When Data Entered)

REPORT DOCUMENTATION PAGE		READ INSTRUCTIONS BEFORE COMPLETING FORM
1. REPORT NUMBER AFOSR-TR- 83-1220	2. GOVT ACCESSION NO. AD-A136247	3. RECIPIENT'S CATALOG NUMBER
4. TITLE (and Subtitle) ION BEAM ASSISTED DEPOSITION OF SiO_2		5. TYPE OF REPORT & PERIOD COVERED Final Report 1 Apr 82 - 31 Dec 82
		6. PERFORMING ORG. REPORT NUMBER
7. AUTHOR(s) John R. McNeil		8. CONTRACT OR GRANT NUMBER(s) AFOSR-82-0165
9. PERFORMING ORGANIZATION NAME AND ADDRESS The University of New Mexico Institute of Modern Optics Albuquerque, NM 87131		10. PROGRAM ELEMENT, PROJECT, TASK AREA & WORK UNIT NUMBERS 61102F 2306/D9
11. CONTROLLING OFFICE NAME AND ADDRESS Air Force Office of Scientific Research/NE Building 410 Bolling AFB, DC 20332		12. REPORT DATE 1983
		13. NUMBER OF PAGES 31
14. MONITORING AGENCY NAME & ADDRESS(if different from Controlling Office)		15. SECURITY CLASS. (of this report) Unclassified
		15a. DECLASSIFICATION/DOWNGRADING SCHEDULE

16. DISTRIBUTION STATEMENT (of this Report)

Approved for public release; distribution unlimited.

17. DISTRIBUTION STATEMENT (of the abstract entered in Block 20, if different from Report)

18. SUPPLEMENTARY NOTES

19. KEY WORDS (Continue on reverse side if necessary and identify by block number)

20. ABSTRACT (Continue on reverse side if necessary and identify by block number)

A Kaufmam ion source was modified to produce a low energy (30 eV) high current dentsity (3 mA/cm^2) O^+ and O_2^+ (O^+/O_2^+) ion beam at an optical surface being coated with SiO_2. Films of SiO_2 were deposited with O^+/O_2^+ ion bombardment at low energy (30 eV) and at high energy (500 eV). Application of the ion-assist technique has the following features:

DD FORM 1 JAN 73 1473 EDITION OF 1 NOV 65 IS OBSOLETE

Unclassified

SECURITY CLASSIFICATION OF THIS PAGE (When Data Entered)

TR-83-1220

Durable coatings can be produced at low substrate temperature.
Film stoichiometry is improved, particularly for low energy bombardment.
Hydrogen content of the film is reduced under certain conditions of bombardment.
Stress and structure of SiO_2 films are not greatly affected by ion bombardment.

ABSTRACT

A Kaufmam ion source was modified to produce al low energy (30 eV) high current density (3 mA/cm^2) O^+ and O_2^+ (O^+/O_2^+) ion beam at an optical surface being coated with SiO_2^n. Films of SiO_2^n were deposited with O^+/O_2^+ ion bombardment at low energy (30 eV) and at high energy (500 eV). Application of the ion-assist technique has the following features:

1) Durable coatings can be produced at low substrate temperature,
2) Film stoichiometry is improved, particularly for low energy bombardment,
3) Hydrogen content of the film is reduced under certain conditions of bombardment, and
4) Stress and structure of SiO_2^n films are not greatly affected by ion bombardment.

TABLE OF CONTENTS

1.0 INTRODUCTION AND BACKGROUND

Ion bombardment of thin films during deposition affects a number of film properties including adhesion, morphology, stoichiometry, stress, impurity content, and packing density [1-4]. Under certain conditions the activation energy necessary for some processes is supplied by the energetic ions, and this reduces the requirements of elevated substrate temperature.

Although bombardment can be accomplished in a number of ways, use of ion beams is advantageous for several reasons. Experimental parameters such as ion current density, ion energy, angle of incidence and ion species are accurately and to a great extent independently controllable. Also, some ion beam techniques can be scaled up for application to large optics. An example is ion-assisted deposition, in which ions bombard a surface being coated by film material generated by a mechanism independent of that of the vapor. The process is limited in scalability by that of the film vapor generation. This is to be contrasted with ion beam sputtering, for example, in which geometries and deposition rates are usually quite restrictive.

The ion beam source used in our laboratory is a Kaufman-type, broad beam, electron bombardment sustained device. This is illustrated in Figure 1. The ion extraction is typically accomplished using a multiple-grid arrangement, and the ion current density is space charge limited [5]. The maximum current density obtainable from the ion source is related to the ion acceleration voltage V and the acceleration distance d by the Child-Langmuir relation

$$J_{MAX} = \left(\frac{2}{me}\right)^{1/2} \frac{V^{3/2}}{9\pi d^2},$$

where m and e refer to the mass and charge of the accelerated particle. In the dual grid arrangement illustrated in Figure 1a, d is approximately the separation between the two grids.

This type of ion source can efficiently generate ion current densities in excess of several mA/cm^2 at 500 V or greater acceleration voltage. However, it has been our experience that such high ion energies can cause film damage (in addition to favorably affecting some film properties) when the ion bombardment is used to assist film deposition. Lower ion energies are desirable to investigate the process further. However, below ~300 V the ion current density available is space charge limited to only a few hundredths mA/cm^2. This current density corresponds to less than one tenth monolayer of bombardment per second, and this is not sufficient for some ion-assisted processes. Practical limits restrict d to approximately 0.5 mm or greater.

A single extraction grid was investigated in this effort to overcome the problems mentioned above. See Figure 1b. Although this arrangement has been discussed previously [6,7], to our knowledge it has not been used to generate O^+ beams for the investigation of ion-assisted deposition of films for optical applications. As discussed in Reference 7, the grid aperture size must be comaprable to or less than the thickness of the plasma sheath ℓ_s for effective operation. The acceleration distance d is now equivalent to ℓ_s. This thickness decreases as V decreases to keep the ion current density equal to the space charge limit.

Over sixty films were deposited in this effort to demonstrate the effects of low energy O^+ bombardment during deposition of SiO_2. Distinct advantages of the low energy process were observed.

In the sections below the experimental arrangement is first described, ion source modification and beam characterization are discussed, and SiO_2 thin film investigations are described.

2.0 EXPERIMENTAL ARRANGEMENT

Figure 2 illustrates the system used for the investigation. A thirty-six inch diameter stainless steel bell jar was used for the deposition of all films. The system was pumped cryogenically and has never been exposed to an oil diffusion pump. The mechanical rough pump was trapped to prevent contamination of the system. Several heat bands maintained the vacuum chamber walls at a temperature of approximately 125 $^{\circ}$ C. Base pressure for the system was approximately 2×10^{-7} Torr. This was most likely limited by the o-ring seals of the system. A Quad 250 residual gas analyzer indicated the major contribution to the background pressure was due to water vapor and nitrogen. The density of these constituents was in a ratio typical for that of a leak-free system. The cryogenic pump could be throttled using a variable shutter assembly. In this manner the chamber pressure could be maintained at some desired level during film deposition.

Figure 2 indicates the orientation of the ion sources used for the deposition process. These sources can be moved and positioned easily and represent a very flexible system. The one source equipped with a dual grid ion extraction system is capable of producing high energy (500 - 2000 eV), high current density (5mA/cm^2) beams of Ar^+ or O^+ at the optic to be coated. This source was used to sputter clean all optics prior to coating as well as to ion-bombard some optics during deposition. The other source was modified in this project to produce low energy (20-50 eV), high current density (2 mA/cm^2) beams of Ar^+ or O^+ at the optic. This is discussed in detail in the section

below. This low energy source was used to ion-bombard some optics during deposition. Both sources have neutralizer attachments. Electrons are emitted that cause the net charge transport of the beam to be zero. This avoids charge buildup while bombarding dielectric materials. The sources can be operated quite independently of each other and represent a unique system for investigation of thin film deposition processes.

Throughout the investigation Faraday probes and a retarding grid analyzer were used to monitor current density actually impinging the optical surface during film deposition. Proper monitoring of the current density at the optical surface during film deposition is important for optimization of ion-assisted deposition.

A rotatable carousel and shutter assembly were used to mount up to four optics at a time in the chamber. In this manner several optics could be coated during one pump-down.

All optics were coated at an ambient temperature of approximately 50 °C. The optics were not rotated during deposition. Resistive heating was used for evaporation of SiO film material. Film thickness was monitored using a crystal oscillator. Deposition rate for all films was approximately 5 Å/sec.

3.0 EXPERIMENTAL RESULTS

3.1 Ion Source Modification for Low Energy Operation.

Figure 1 illustrates the arrangement of the Kaufman-type ion source used in the investigation. Both dual grid and single grid arrangements are indicated. Grid diameter of both sources was 2.5 cm. The single grid design was arranged by replacing the dual grid system with a single layer of thin mesh. Several materials were investigated, with performance improving as the grid thickness was decreased. See the discussion in Sec. 1.0. It was found that Ni

mesh of approximately 0.4 mm aperture size was most satisfactory. Cathode and neutralizer filaments were W. Efficient ion extraction was observed for ion energies as low as 30 eV.

Typical operating parameters to generate a 30 eV oxygen beam are:

chamber pressure ~ $1\text{-}10 \times 10^{-5}$ Torr (variable)

gas flow rate through source ~ 3 sccm

discharge voltage 60V

discharge current 0.5 - 1.5 A

grid voltage -10 V

anode voltage 30 V

grid current 2 mA

beam current 15 mA

beam current density at grid 3.8 mA/cm^2

beam current density 15 cm from grid 1.7 mA/cm^2

Note that the current density downstream of the ion source fluctuates considerably with chamber pressure and gas flow rate. Similar conditions are used to produce an argon beam.

A retarding grid analyzer was constructed and used to measure the ion beam current density and energy distribution. Figure 3a illustrates the probe arrangement. Note that multiple retarders were used to minimize secondary electron emission due to ion bombardment of the analyzer and thus to avoid erroneous probe readings. The probe detector was biased at -27 V, and the surrounding probe body was at ground potential. The three retarder grids were biased by voltage-dividing a positive ramp output from an oscilloscope. Probe current was converted to a voltage, amplified and displayed on the oscilloscope screen.

Figure 3b shows results of analyzing a 40 eV O^+ beam. In the photograph of the oscilloscope trace, the upper trace displays probe signal, and the lower trace displays the retarding voltage on the analyzer. It can be seen that the probe signal is relatively constant for retarding voltages less than approximately 35 V; between 35 and approximately 40 V the probe signal decreases; at retarding voltages greater than approximately 40 V the probe signal is zero. This confirms virtually all of the ions in the 40 eV beam have energy less than 40 eV and greater than approximately 35 eV.

This fact is significant. Other investigators of low energy O^+ ion-assisted deposition [8] have demonstrated benefits of the process. However, the ion sources employed have a broad distribution of ion energies, with some ions of energy exceeding 100 eV. It is believed [8] this fraction at higher energy is responsible for undesirable film properties observed. The ion source modified in this effort should not produce such problems.

The analyzer results are generally consistent with Langmuir probe theory. The relationship between the second derivative of probe current J(V) and the ion energy distribution function F(V) is expressed as [9]

$$\frac{d^2J}{dV^2} = \frac{K}{\sqrt{V}} F(V)$$

where K is a constant, and V is the ion accelerating in one direction ($V_{\parallel}$ in Figure 3a). If the beam current were composed of monoenergetic ions traveling only along $v_{\parallel}$ and the probe were infinite, the probe current would decrease sharply at voltage V.

There are two possible explanations for the probe current not decreasing sharply. The ions are emitted with a $V_{\perp}$ velocity component (see Figure 3a), as

determined by spatially mapping the beam current. This would cause the probe current to decrease with voltage V as

$$V = \frac{1}{2} \frac{M}{e} \bar{v}^2 \cos^2 \theta$$

with θ having values between 0 and $\theta_0 \approx 30^\circ$. The probe diameter (~0.5 cm) and ion beam source diameter (2.5 cm) are sufficiently small compared to the separation between ion source and probe (15 cm) such that effects of experimental geometry on angle θ above are most likely negligible. If the ion energy were not monoenergetic ($\Delta v \neq 0$ in Figure 3a), the probe current would not decrease sharply. One possible cause for this would be the temperature of the ions and neutral atoms in the discharge region. If, in the worst case, the probe behavior were due entirely by an energy spread of beam ions, the spread would amount to only approximately 5 eV. For applications of the ion beam in our work, this is insignificant.

3.2 Effects of Low Energy O^+ Bombardment of SiO_2 Films

The second part of this effort involved demonstrating the effects of low energy O^+ bombardment during the deposition of SiO_2 films. The starting material for the SiO_2 films was SiO. This material was chosen for two reasons. First, the material is important as a low-index film in multilayer structures. Applications for this material range from ultraviolet through near infrared wavelengths. Second, SiO can be evaporated using resistively heated sources and is one of few oxide materials for which this is practical. Although we now have an electron beam apparatus, at the start of this effort we did not.

Note that SiO_2 can be evaporated well from an electron beam source, and this technique can be considered a benchmark for comparison. As such, use of SiO as a starting material for SiO_2 represents a worst case for testing the effectiveness of O^+ bombardment for improving optical characteristics of films.

Coatings were deposited under a variety of experimental conditions. Ion beam current density at the optic ranged from 0 to over 1 mA/cm^2. Beam energies of 30 eV and 500 eV were employed. Pressure of oxygen ranged from approximately $2x10^{-7}$ through $2x10^{-4}$ Torr. It was found that films deposited at higher pressure were fragile and were easily damaged by cleaning. Films deposited at an O_2 pressure of approximately $3x10^{-5}$ Torr were hard and robust. Because the oxygen flow through the ion source was directed toward the optic, the density at the optical surface could have been several times that corresponding to the chamber pressure of $3x10^{-5}$ Torr. Film deposition rate was held constant at approximately 5 Å/sec. The relative arrival rates of O^+, O_2, and SiO were thus varied over a wide range of values.

Note that a SiO_2 deposition rate of 5 Å/sec corresponds to an arrival rate of approximately 2×10^{15} $(cm^2\text{-sec})^{-1}$. Similarly, an O_2 current density of 100 $\mu A/cm^2$ produces a flux of 0.6×10^{15} $(cm^2\text{-sec})^{-1}$, and a pressure of O_2 of 3×10^{-5} Torr produces a flux of approximately 1×10^{16} $(cm^2 - sec)^{-1}$ at the optical surface.

3.2.1 Optical Analysis

Analysis of the films' optical transmission characteristics was used to assess the effects of O^+ bombardment on stoichiometry. The films were deposited on fused silica that was a good uv-grade. By examining the short wavelength cutoff in transmission of the film compared to that of the bulk (uncoated substrate), a measure of the film stoichiometry can be obtained [8].

Figure 4 shows the transmittance of several films of approximately 400 nm physical thickness. Beam energy of the O^+ ions was 500 eV. The advantage of bombardment is clear, and can be seen by comparing the film transmittance for no bombardment (J=0) to that for bombardment present during deposition. Notice that the transmittance approaches that of the uncoated substrate for increasing bombardment current density, up to a level of approximately 15 $\mu A/cm^2$. For current density greater than this value, there is clearly a departure in the transmittance characteristics of the substrate and film.

The film material for the case of J=0 is most likely a mixture of SiO, SiO_2 and Si_2O_3 [8,10,11]. As current density at the optical surface of O^+ increases, a larger fraction of the molecules become oxidized to form SiO_2. However, there is apparently a competing mechanism that results in the optimal level of O^+ current density. A likely damage mechanism from the 500 eV O^+ beam is due to sputtering of the SiO_2 film material. The different sputtering rates for the two elements, with oxygen being preferentially removed, could produce an altered layer that is integrated into the film as deposition proceeds. Preferential sputtering damage has been observed for several oxide materials bombarded with Ar^+ ions [12,13,14]. For our situation, the damage mechanism dominates the beneficial effects of increased oxidation for current density at the optical surface in excess of approximately 15 $\mu A/cm^2$.

Figure 5 shows the results of using a 30 eV beam of O^+ ions to bombard the optic during deposition. Here, too, the transmittance of the films approaches that of the bulk for increasing levels of bombardment. However, the films transmittance more closely approaches that of the the bare substrate for this low energy case, up to an O^+ density of approximately 75 $\mu A/cm^2$. For greater current density, the departure of the film and substrate transmittance

characteristics are less apparent than in the case of 500 eV O^+ bombardment. The competing mechanism in this low energy case is not as effective, as might be expected if the mechanism is due to preferential sputtering by O^+.

Figure 6 summarizes data from Figures 4 and 5 by comparing the optical transmittance of the films at an arbitrary wavelength of 250 nm. The difference in transmittance between the bare fused silica substrate and the film plus the substrate is plotted versus O^+ current density at the optical surface. For 30 eV O^+ bombardment, the value of $(T_{SUB}-T)$ more closely approaches zero and varies with current density more slowly than in the case of 500 eV O^+ bombardment.

It is noteworthy that all films discussed above were deposited on substrates at ambient temperature ($\approx 50^\circ C$). Hard, durable films were obtained when O^+ bombardment was employed. As a test to examine the effect of substrate temperature, samples were coated at a substrate temperature of approximately 250 °C. Figure 7 summarizes the results. When ion bombardment is employed, there is little difference in optical transmittance between films deposited on heated and unheated substrates. Without using ion bombardment, there appears to be a lower oxygen content in films deposited on heated substrates. This has been observed by other investigators [8].

Figure 8 compares the best sample from Figure 5 with a sample coated using electron beam evaporation of SiO_2. This second sample was deposited on a substrate heated to approximately 250 °C. The transmittance of this electron beam deposited sample was slightly less than that of the O^+ bombarded sample deposited on a substrate at ambient temperature.

3.2.2 H Content in Films

Atomic hydrogen content in films produces undesirable mechanical effects in films, such as causing the film to be brittle. Filaments and deposition boats constructed of W are potential sources of H. If present in

the form of H_2O, optical absorption can be increased, index if refraction is changed, and the film often becomes less durable. When films are exposed to air, H_2O is absorbed, and this is usually irreversible. The severity of the H_2O problem is often connected with the porousity of the film structure, as in the case of ThF_4. More recently H_2O content in SiO_2 films has been attributed to film porousity [14].

Recently it has been reported that film materials which strongly getter 0 during depostion also tend to have a high concentration of H incorporated into the film. Atomic percentages of H of 15% or greater were reported for the deposition of Cr_2O_3. Part of the oxygen that was gettered is believed to have come from residual water vapor in the vacuum system. The residual hydrogen content in the system increased sharply during deposition, resulting in a high concentration incorporated in the film.

Our deposition of SiO_2 using SiO as a starting material is similar to the situation just described. Because of this, several films were examined for H-content using the technique of elastic recoil detection. This involves the detection of H forward scattered by 2.4 MeV He incident on the target. The process is described in Reference 16. Spatial resolution of approximately 300 Å in the film is possible, with a sensitivity of H of 0.1%.

Figure 9 illustrates the results of the elastic recoil measurements of several samples. Content of H is plotted versus O^+ bombardment current density. The values plotted for each level of current density represent an average value of H content in the film. There appears to be a decrease in H content for beam energy of 500 eV, with nearly a factor of 10 difference in content between the film deposited with no bombardment and the film deposited with $J = 225\mu A/cm^2$. In the case of 30 eV beam energy, there is perhaps a decrease in H content by a

factor of 2 due to bombardment. Figure 10 illustrates the spatial variation of H content throughout the two film samples with most and least concentrations.

Note that only seven coating were investigated to obtain the H concentration, and firm conclusions should not be drawn based only on this information. The form of H in the film can not be determined from this information alone. Spectroscopic information in the near infrared is required. The decrease in H content illustrated in Figure 9 is due either to preferential sputtering, or it is a result of the film structure becoming more dense with increased bombardment. The distribution shown in Figure 10 might suggest diffusion is not the case. However, the larger concentration of H near the film/substrate interface is not understood.

3.3.3 Film Stress and Structure

Film stress is often explained in connection with the columner structure of the film. Because of this, these two aspects are discussed together.

Film stress was investigated by measuring the deformation of a thin (0.010^{11}) fused silica sample of 1 inch diameter. This was done using interferometry, and the analysis follows the treatment by Roll [17]. The treatment assumes isotropic, homogeneous stress distribution in the coating in which deformations of the substrate are small compared to substrate thichness.

Films of 1.5μ and 0.4μ thichness were examined with different levels of bombardment and substrate temperature. Results are shown in Table 1. In general it can be seen that all films had a compressive stress that was slightly reduced due to bombardment. Substrate temperature and bombarding O^+ ion energy had little effect that was detectable from the data shown.

It is interesting that the compressive stress was reduced due to ion bombardment. This could be indicative of a stress relief mechanism initiated by

ion bombardment. In different situations, ion bombardment has resulted in an increase in compressive stress (or decrease in tensile stress) due to an "ion stuffing" effect.

Film structure was examined by cleaving thin Si samples that had thick films. The side view of the sample was then examined using a scanning electron microscope (SEM). This technique is commonly used to try to observe film morphology. We observed no film structure, even for films 4μ thick deposited without ion bombardment. This is consistent with the generally accepted notion that SiO_2 films are amorphous in structure.

4.0 CONCLUSIONS

The ion source modification was successful, and we now have a useful, unique capability to investigate effects of thin film bombardment during deposition. Application of O^+ bombardment during deposition of SiO_2 has the following attractive features:

A. Durable coatings can be produced at low substrate temperature.

B. Film stoichiometry is improved, particularly for low energy (30 eV) ion bombardment.

C. Hydrogen content of the film is reduced under high energy (500 eV) ion bombardment, and possibly in the case of low energy bombardment.

D. Stress and structure of SiO_2 films are not greatly affected by ion bombardment; other film materials are greatly effected.

The first item can have particular application in coating large optics, for which it is undesirable and difficult to heat the substrate.

These results suggest several more fundamental problems. The nucleation and growth of thin films are influenced by ion bombardment, and knowledge of these processes is sparse. The same can be said concerning the optical and

mechanical properties of films. The damage mechanism connected with ion bombardment is of direct importance to improving film quality. Perhaps photon bombardment could be used as a mechanism to deliver energy to the film surface but yet avoid some of the effects associated with ion bombardment, such as dislocations or sputtering. This could possibly be a way to begin sorting out some mechanisms.

REFERENCES

1. W. C. Herrmann, Jr. and J. R. McNeil, SPIE Conference on Optical Thin Films, Vol. 325, Jan. 26, 1982, Los Angeles, CA.
2. T. Spalvins, J. Vac. Sci. Technol. 17, 315 (1980).
3. R. D. Bland, G. J. Kominiak, and D. M. Mattox, J. Vac. Sci. Technol., 11, 671 (1974).
4. E. H. Hirsch and I. K. Varga, Thin Solid Films, 52, 445 (1978).
5. H. R. Kaufman, J. Vac. Sci. Technol., 15, 272 (1978).
6. P. Le Vaguerese and D. Pigache, Rev. Phys. Appl. 6, 325 (1971).
7. J. M. E. Harper, M. Heiblum, J. L. Speidell, and J. H. Cuomo, J. Appl. Phys. 52, 4118 (1981).
8. J. Ebert, SPIE Conference on Optical Thin Films, Vol. 325, Jan 26, 1982, Los Angeles, Ca.
9. J. D. Cobine, Gaseous Conductors, Dover, 1958.
10. E. Ritter, Opt. Acta. 9, 197 (1962).
11. T. H. Allen, Conference on Optical Thin Films, Vol. 325, Jan. 26, 1982, Los Angeles, Ca.
12. P. H. Holloway and G. C. Nelson, J. Vac. Sci. Technol., 16, 783 (1979).
13. R. Kelly, Nucl. Instrum. Methods 149, 553 (1978).
14. P. J. Martin, H. A. Macleod, R. P. Netterfield, C. G. Pacey, and W. G. Sainty, Appl. Opt., 22, 178 (1983).
15. J. J. Cuomo, personal communication.
16. B. L. Doyle and P. S. Peercyy, Appl. Phys. Lett. 34, 811 (1979).
17. K. Roll, J. Appl. Phys., 47, 3224 (1976).

FIGURE CAPTIONS

Figure 1: Kaufman ion source used in this investigation, with conventional dual grid extraction (a) and single grid extraction arrangement (b).

Figure 2: Experimental arrangement used in this investigation.

Figure 3: (a) Probe arrangement used to energy analize ion beam; (b) probe current versus retarding voltage.

Figure 4: Transmittance of SiO_2 films on fused silica for 500 eV O^+ bombardment at different current densities. Film thickness in all cases is approximately 4000 Å.

Figure 5: Transmittance of SiO_2 films on fused silica for 30 eV O^+ bombardment at different current densities. Film thickness in all cases is approximately 4000 Å.

Figure 6: Optical transmittance at 250 nm of films illustrated in Figures 4 and 5.

Figure 7: Comparison of transmittance of films deposited at ambient temperature ($\approx$ 50 °C) and at 250 ° C, with and without ion bombardment.

Figure 8: Transmittance of SiO_2 films deposited using e-beam and ion-assisted techniques.

Figure 9: H content of SiO_2 films deposited under different amounts of O^+ ion bombardment; amounts shown represent a spatial average throughout the film.

Figure 10: H content of SiO_2 films, showing variation throughout the film. Two samples were those having the most and least concentration shown in Figure 9.

TABLE 1

Film Thickness	J(μA/cm^2)	E_B(eV)	T_{SUB}(°C)	Stress(dy/cm^2)
1.5μ	0	30	$\approx$ 50	7.5×10^{-9}
1.5μ	135	30	$\approx$ 50	6.1×10^{-9}
1.5μ	240	30	$\approx$ 50	6.2×10^{-9}
0.4μ	0	700	$\approx$ 50	14×10^{-9}
0.4μ	120	700	$\approx$ 50	11×10^{-9}
0.4μ	0	700	$\approx$ 250	19×10^{-9}
0.4μ	120	700	$\approx$ 250	16×10^{-9}

TABLE 1: Summary of film stress measurements for different O^+ bombardment during deposition. All films had compressive stress.

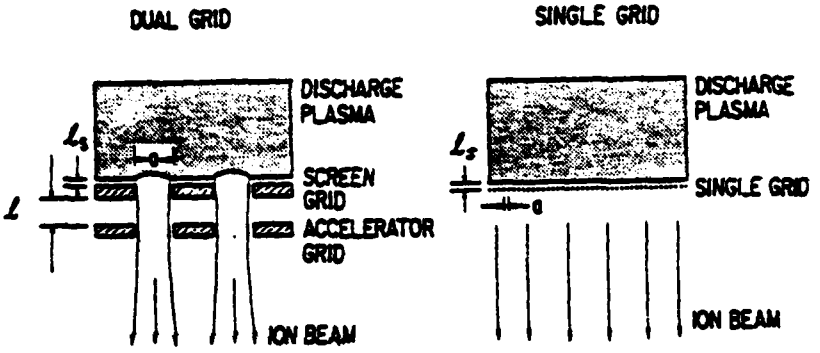

Figure 1. Kaufman ion source used in this investigation, with conventional dual grid extraction (a) and single grid extraction arrangement (b).

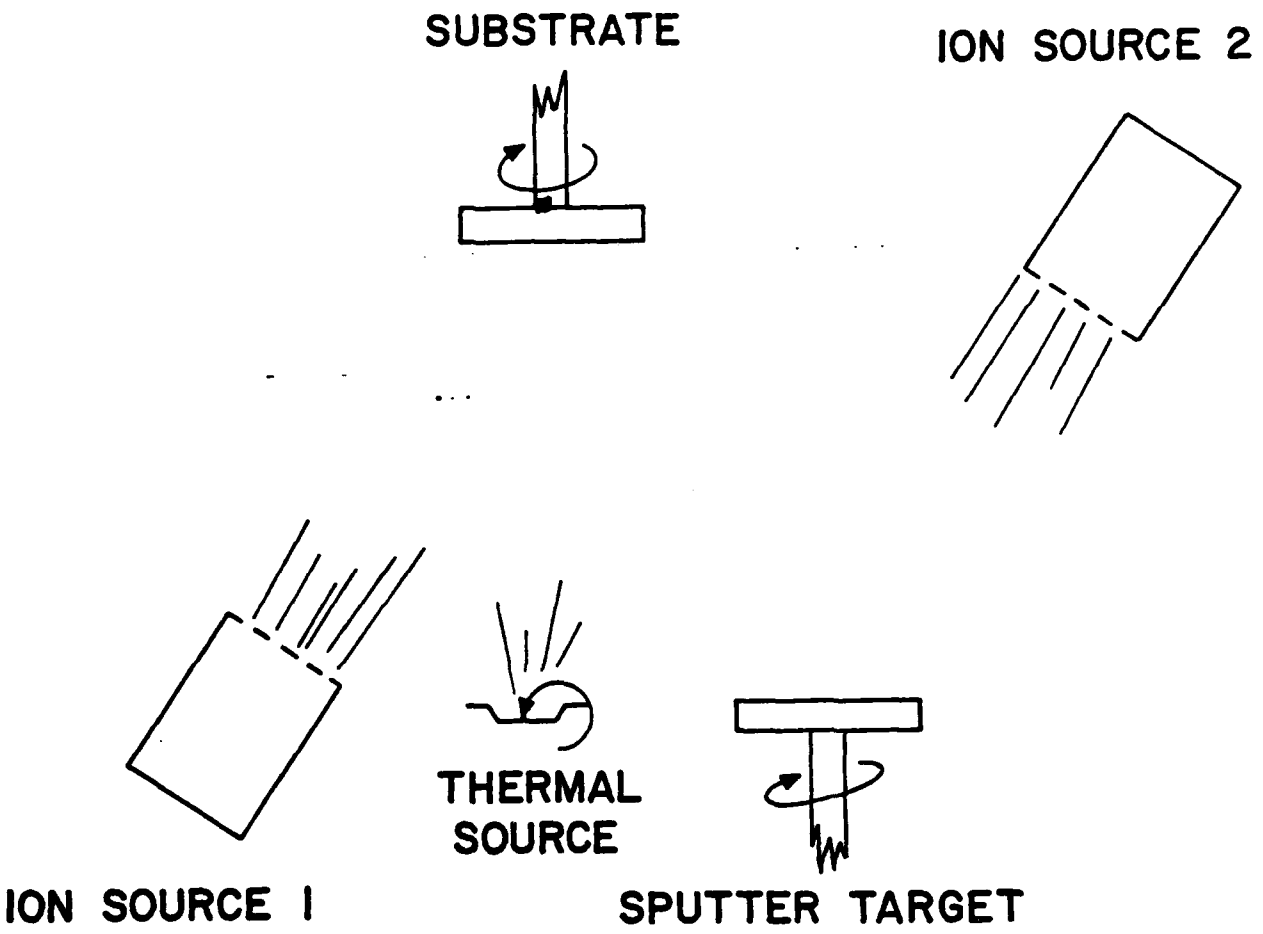
SUBSTRATE
ION SOURCE 2
THERMAL
SOURCE
ION SOURCE 1
SPUTTER TARGET

Figure 2

a.)

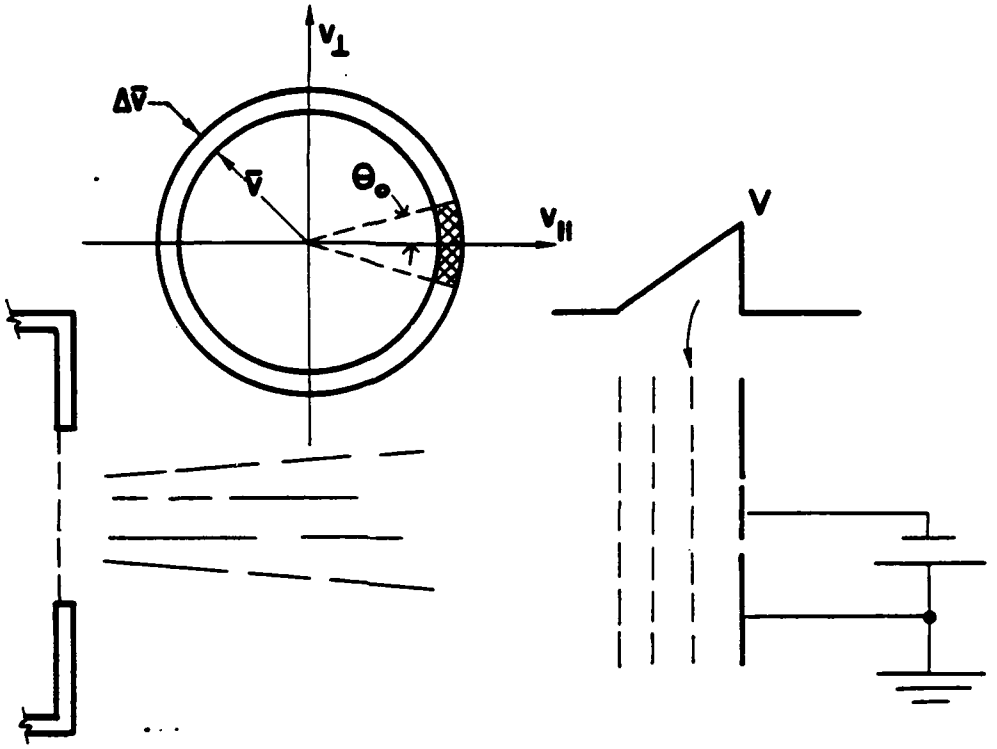
$v_\perp$
$\Delta\bar{v}$
$\bar{v}$
θ_o
$v_{||}$
V

b.)

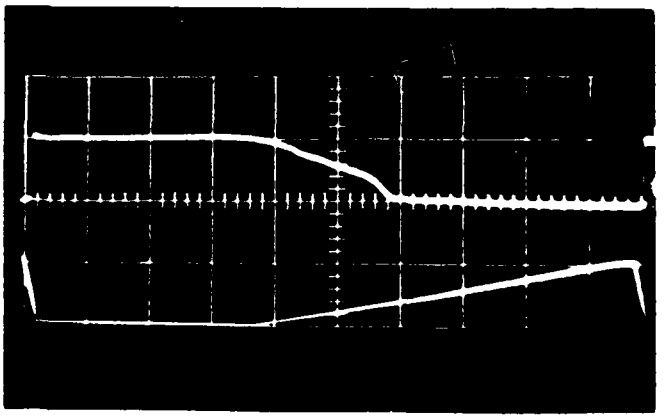
PROBE CURRENT
RETARDING VOLTAGE
100V/DIV
TIME

Figure 3

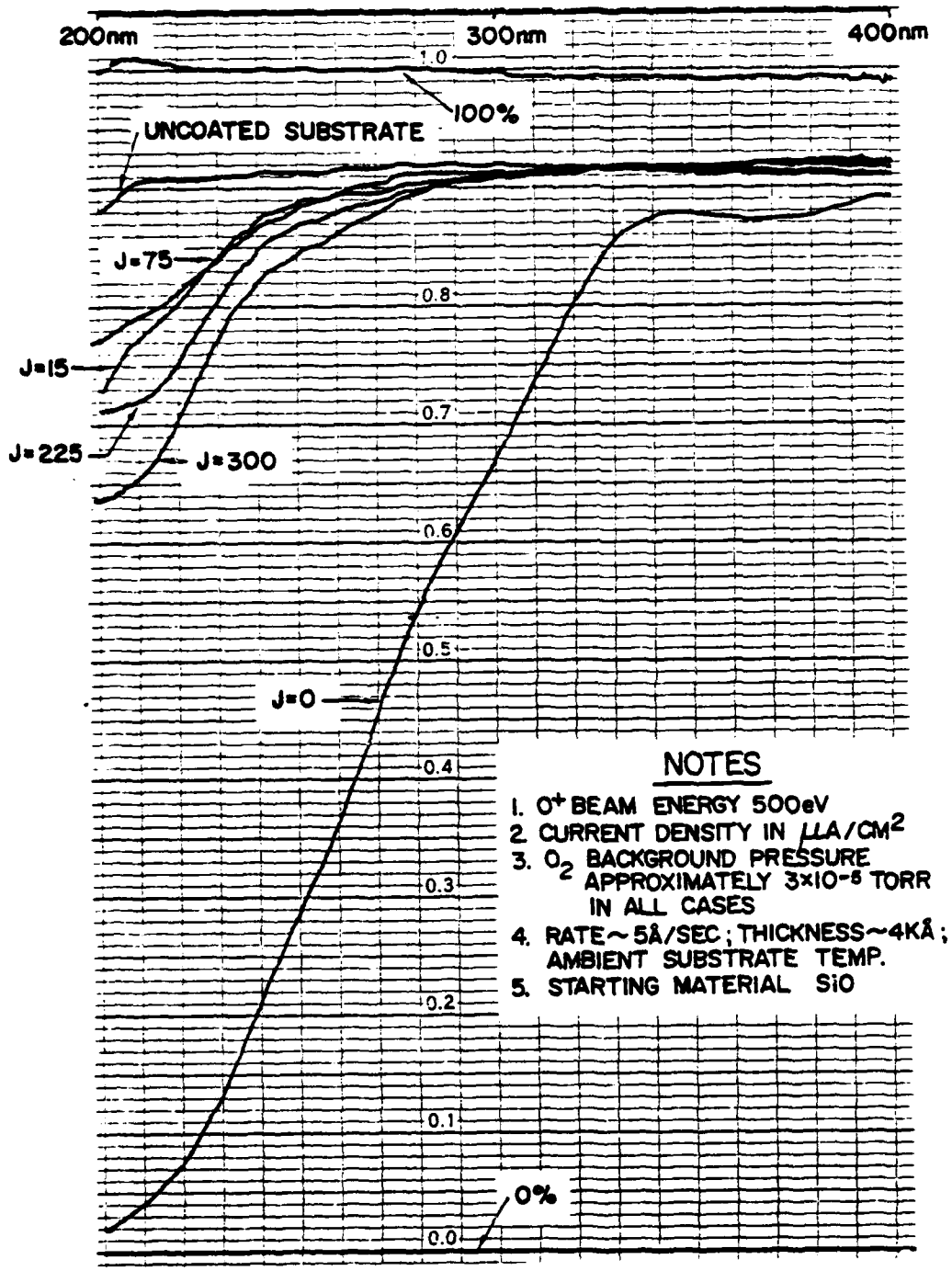

4. Transmittance of SiO_2 films on fused silica for 500 eV O^+/O_2^+ bombardment at different current densities. Film thickness in all cases is approximately 4000 Å.

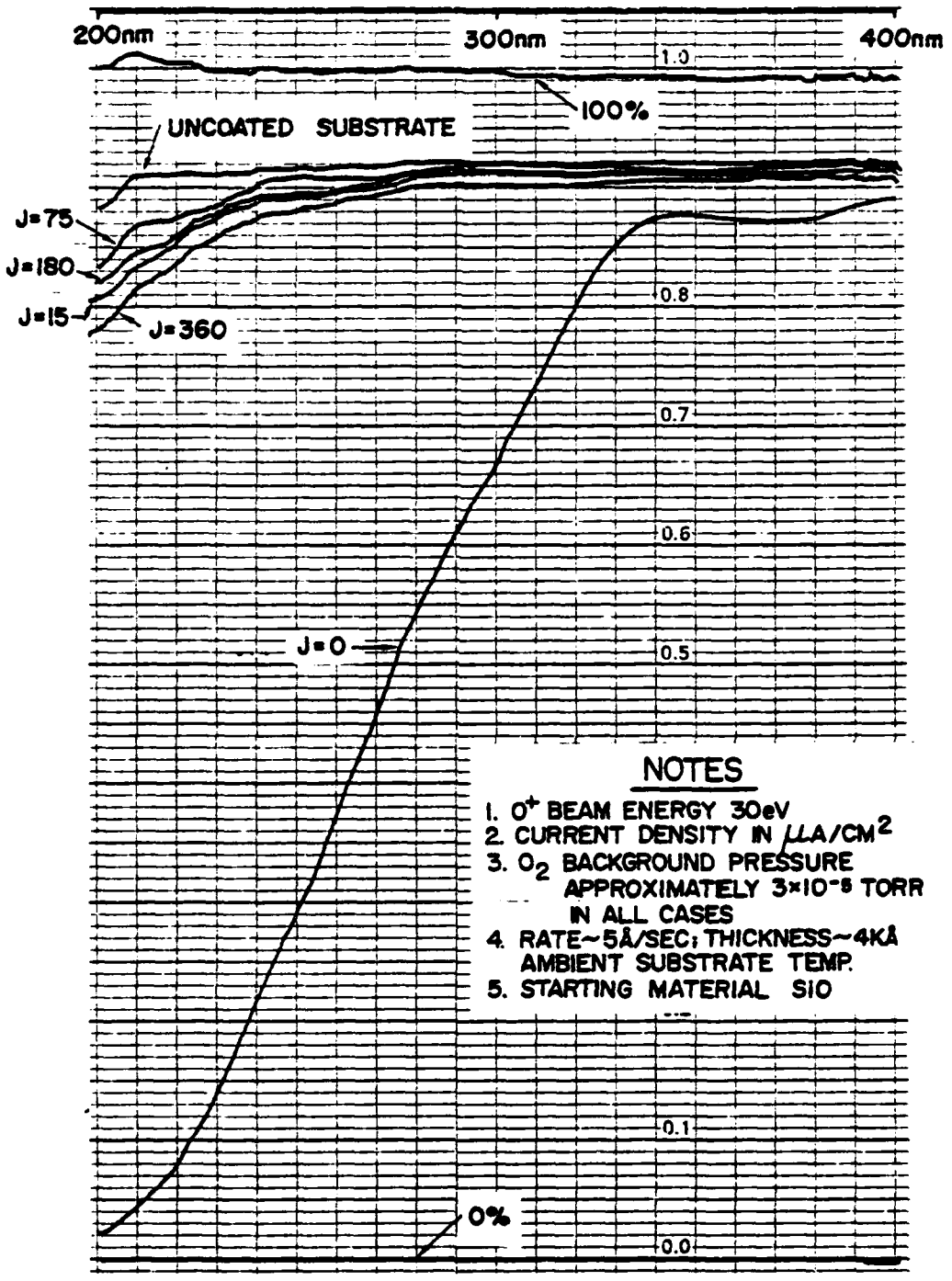

5. Transmittance of SiO_2 films on fused silica for 30 eV O^+/O_2^+ bombardment at different current densities. Film thickness in all cases is approximately 4000 Å.

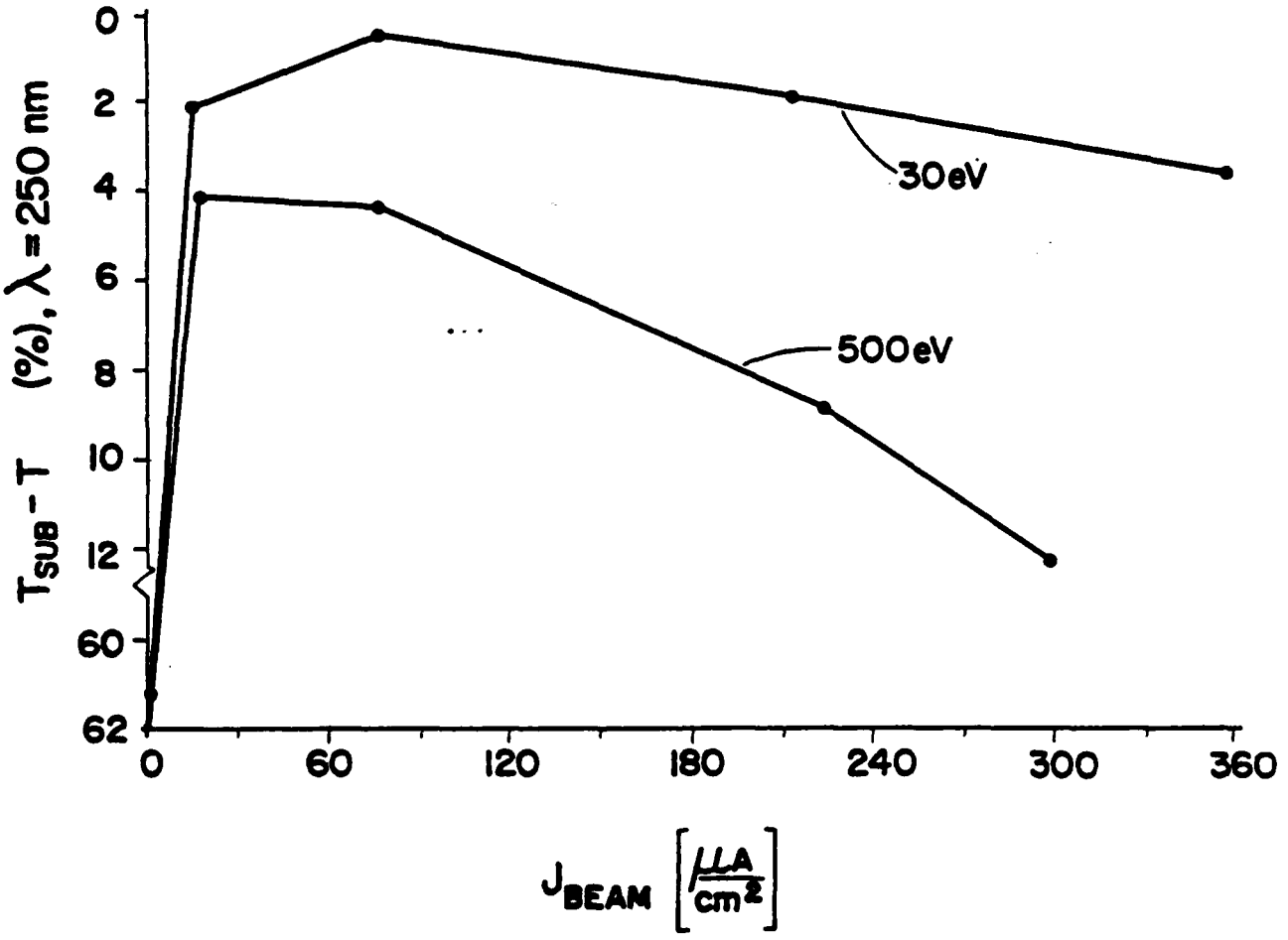

6. Optical transmittance at 250 nm of SiO_2 films illustrated in Figures 3 and 4.

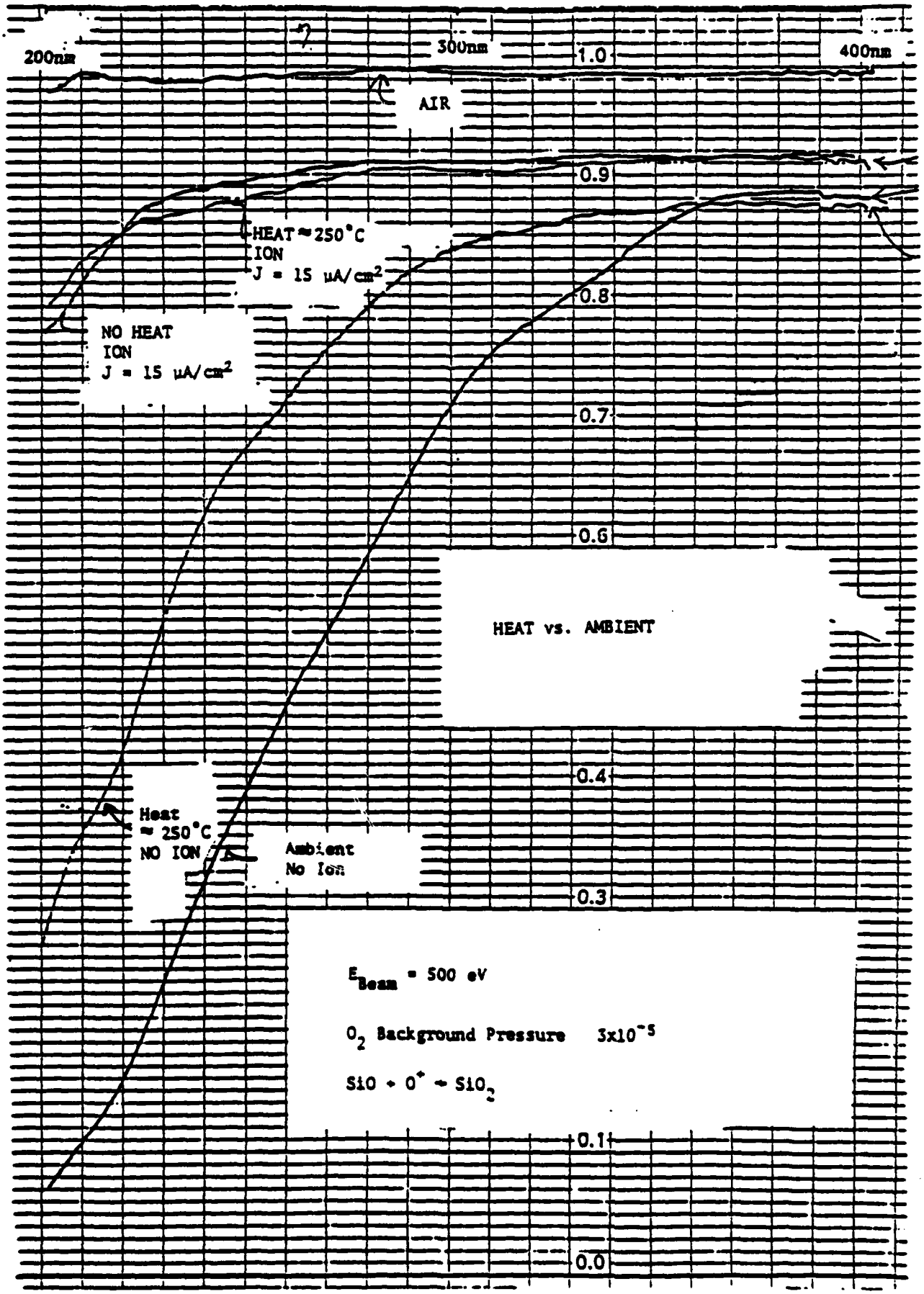
200nm
300nm
400nm
1.0
0.9
0.8
0.7
0.6
0.4
0.3
0.1
0.0
AIR
HEAT ≈ 250°C
ION
J = 15 μA/cm²
NO HEAT
ION
J = 15 μA/cm²
HEAT vs. AMBIENT
Heat
≈ 250°C
NO ION
Ambient
No Ion
E Beam = 500 eV
O2 Background Pressure 3x10⁻⁵
SiO + O⁺ → SiO2

Figure 7

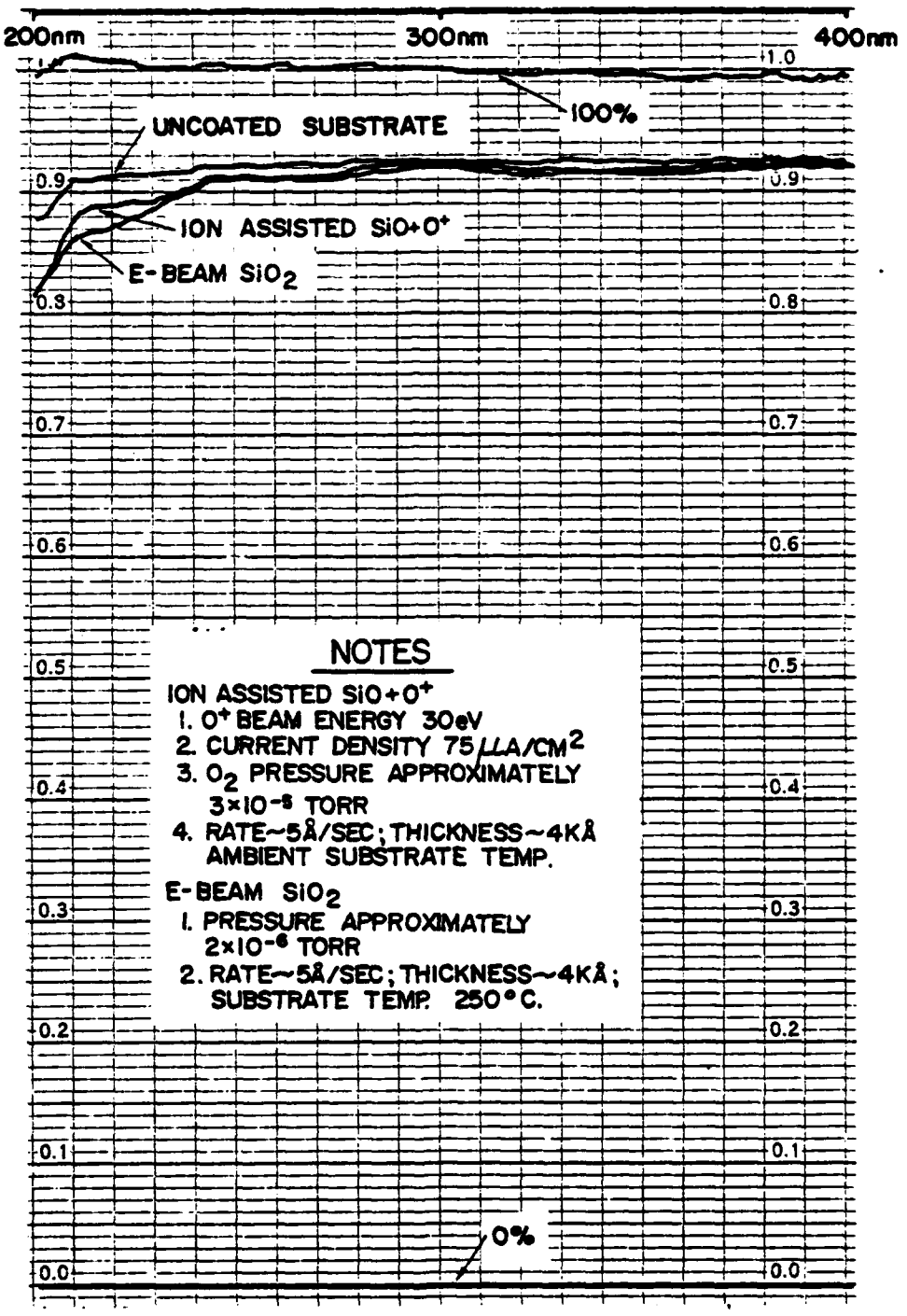

8. Transmittance of SiO_2 films deposited using e-beam and ion-assisted techniques.

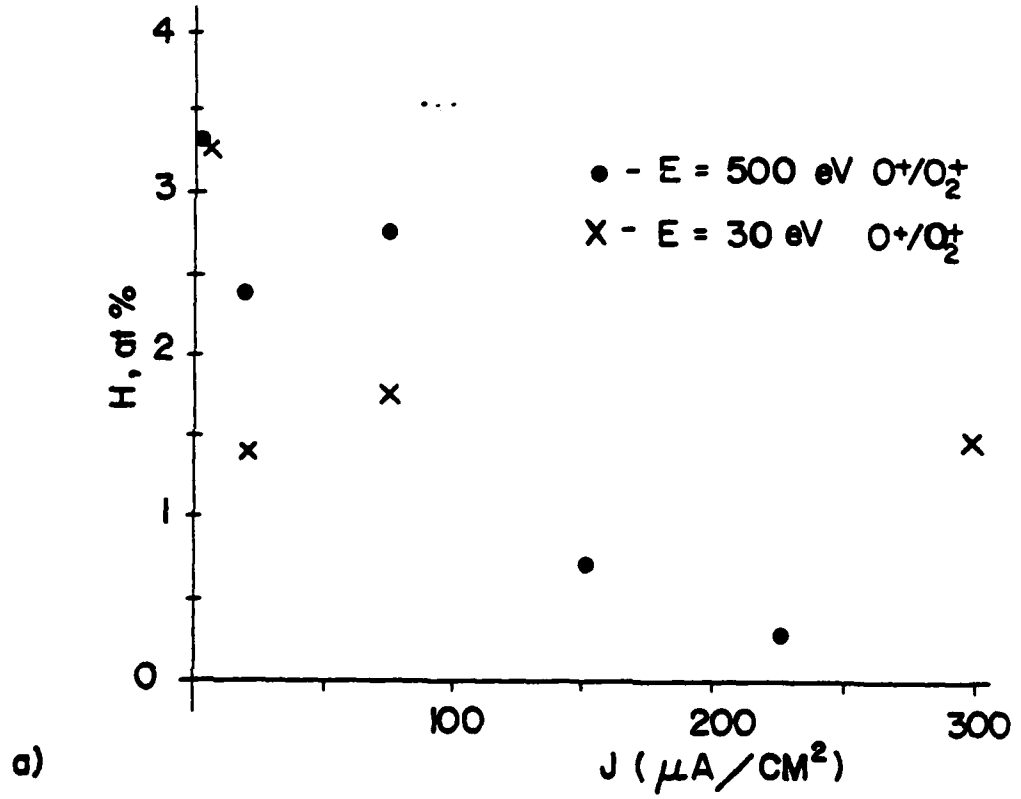

9. Average atomic percent of H content in ion bombarded SiO_2 films.

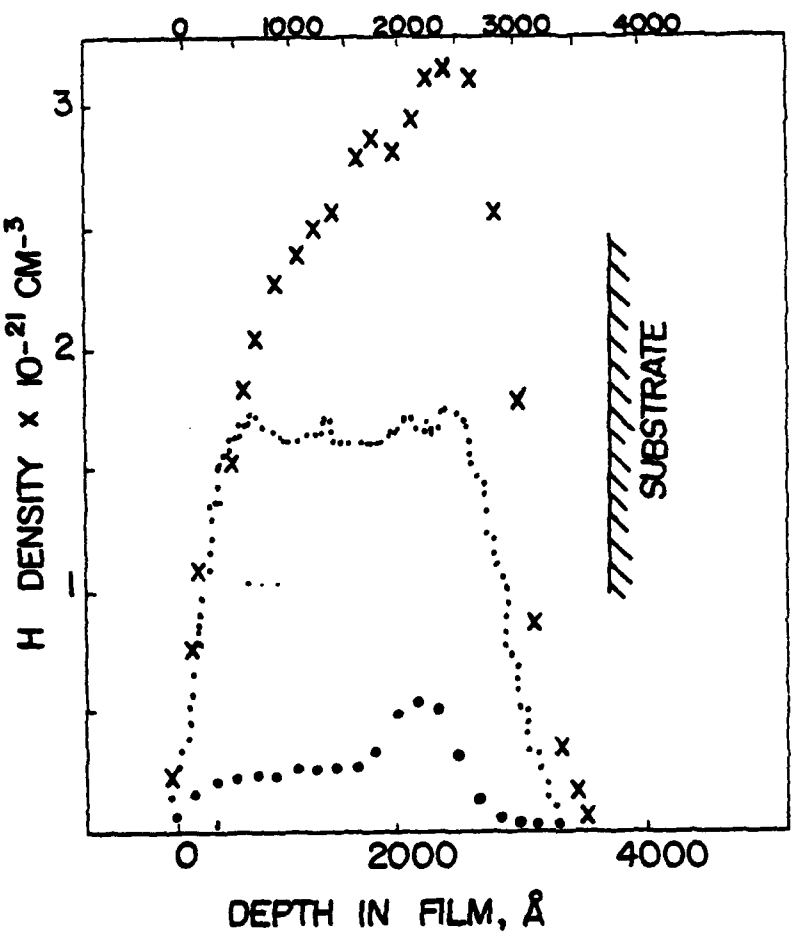

b)

10. Spatially resolved measurements of H content in films with the least, most, and moderate amounts of H (illustrated in part a).